wing. This effect persisted in the front part of the wing as well (until about a 50-deg angle of attack) even though all four wing shapes had the same sweep-back angle at the apex. Additional details of the static condition results are presented by Myose et al.[19]

Figure 2 compares the vortex breakdown locations for the four different wing shapes at a given pitch rate. The breakdown locations are given in terms of percentage of chord measured from the wing apex. Thus, a breakdown location of 0% corresponds to full stall where the leading-edge vortices are completely burst. The region below each curve corresponds to a condition where the vortex is not burst. It is desirable for this region to be as large as possible, because this is the area where enhanced lift from the vortical flow is still present.

The solid curves in Fig. 2 compare the pitch-up results. Like the static case, the double-delta wing had the earliest vortex breakdown location under pitch-up. Among the four shapes tested, the cropped wing had the longest unburst vortex. There appear to be two parallel sets of vortex breakdown curves. The first set, belonging to wings with aft sweep-back angles greater than or equal to 90 deg (i.e., cropped and diamond wings), have vortex breakdown curves that tend to be roughly linear with angle of attack. The second set, belonging to wings with aft sweep-back angles less than 90 deg (i.e., delta and double-delta wings), have vortex breakdown curves that tend to have a convex–concave shape.

The dashed curves in Fig. 2 compare the vortex breakdown locations for the four different wing shapes at a given pitch-down rate. The double-delta wing had the earliest vortex breakdown and the cropped wing had the longest unburst vortex. The slower ($\kappa = 0.05$ and 0.10) pitch-down results appear to show two parallel sets of vortex breakdown curves. The first set of curves is concave and belongs to wings with aft sweep-back angles greater than or equal to 90 deg. The second set of curves has a slight kink and belongs to wings with aft sweep-back angles less than 90 deg.

Although not shown here, the longest unburst vortex during pitch-up was obtained at the fastest pitch rate.[19] Conversely, the slowest pitch rate provided the longest unburst vortex during pitch-down. This is consistent with the results of previous studies on delta wings under dynamic conditions.[12,14,15]

Summary

The effect of delta wing shape on leading-edge vortex breakdown was investigated in the 2 × 3 ft water tunnel at Wichita State University. In this experiment, the aft one-third of a 76-deg swept delta wing was modified to obtain diamond, cropped, standard delta, and double-delta shapes. The vortex breakdown location during dynamic pitch-up and pitch-down motion was observed by dye flow visualization. Among the four shapes tested, the cropped delta wing had the longest unburst leading-edge vortex during dynamic pitching and the double-delta wing had the earliest vortex breakdown.

Acknowledgments

The authors are grateful for the assistance of Arthur Porter, Ping-Chian Yeong, and the Beech wind tunnel staff supervised by Bonnie Johnson.

References

[1]Polhamus, E., "A Concept of the Vortex Lift of Sharp-Edge Delta Wings Based on a Leading-Edge Suction Analogy," NASA TN D-3767, Dec. 1966.

[2]Earnshaw, P. B., and Lawford, J. A., "Low-Speed Wind Tunnel Experiments on a Series of Sharp-Edged Delta Wings," Aeronautical Research Council, RM No. 3424, 1964.

[3]Erickson, G. E., "Water-Tunnel Studies of Leading-Edge Vortices," *Journal of Aircraft*, Vol. 19, No. 6, 1982, pp. 442–448.

[4]Seginer, A., and Salomon, M., "Performance Augmentation of a 60-Degree Delta Aircraft Configuration by Spanwise Blowing," *Journal of Aircraft*, Vol. 23, No. 11, 1986, pp. 801–807.

[5]Wood, N. J., and Roberts, L., "Control of Vortical Lift on Delta Wings by Tangential Leading-Edge Blowing," *Journal of Aircraft*, Vol. 25, No. 3, 1988, pp. 236–243.

[6]Parmenter, K., and Rockwell, D., "Transient Response of Leading-Edge Vortices to Localized Suction," *AIAA Journal*, Vol. 28, No. 6, 1990, pp. 1131–1133.

[7]McCormick, S., and Gursul, I., "Effect of Shear Layer Control on Leading Edge Vortices," AIAA Paper 96-0541, Jan. 1996.

[8]Marchman, J. F., "Aerodynamics of Inverted Leading-Edge Flaps on Delta Wings," *Journal of Aircraft*, Vol. 18, No. 12, 1981, pp. 1051–1056.

[9]Karagounis, T., Maxworthy, T., and Spedding, G. R., "Generation and Control of Separated Vortices over a Delta Wing by Means of Leading Edge Flaps," AIAA Paper 89-0997, March 1989.

[10]Gursul, I., Yang, H., and Deng, Q., "Control of Vortex Breakdown with Leading-Edge Devices," AIAA Paper 95-0676, Jan. 1995.

[11]Hayashibara, S., Myose, R. Y., and Miller, L. S., "The Effect of a 70° Swept Canard on the Leading-Edge Vortices of a 70° Swept Delta Wing During Dynamic Pitching," AIAA Paper 97-0613, Jan. 1997.

[12]Myose, R. Y., Hayashibara, S., Yeong, P. C., and Miller, L. S., "The Effect of Canards on Delta Wing Vortex Breakdown During Dynamic Pitching," *Journal of Aircraft* (to be published).

[13]Lee, M., and Ho, C. M., "Lift Force of Delta Wings," *Applied Mechanics Review*, Vol. 43, No. 9, 1990, pp. 209–221.

[14]Miller, L. S., and Gile, B. E., "Effects of Blowing on Delta Wing Vortices During Dynamic Pitching," *Journal of Aircraft*, Vol. 30, No. 3, 1993, pp. 334–339.

[15]LeMay, S. P., Batill, S. M., and Nelson, R. C., "Vortex Dynamics on a Pitching Delta Wing," *Journal of Aircraft*, Vol. 27, No. 2, 1990, pp. 131–138.

[16]Wentz, W. H., and Kohlman, D. L., "Vortex Breakdown on Slender Sharp-Edged Wings," *Journal of Aircraft*, Vol. 8, No. 3, 1971, pp. 156–161.

[17]Gatlin, G. M., and McGrath, B. E., "Low-Speed Longitudinal Aerodynamic Characteristics Through Post-Stall for Twenty-One Novel Planform Shapes," NASA TP-3503, 1995.

[18]Grismer, D. S., and Nelson, R. C., "Double-Delta-Wing Aerodynamics for Pitching Motion With and Without Sideslip," *Journal of Aircraft*, Vol. 32, No. 6, 1995, pp. 1303–1311.

[19]Myose, R. Y., Lee, B. K., Hayashibara, S., and Miller, L. S., "An Experimental Study on the Breakdown of Leading-Edge Vortices on Diamond, Cropped, Delta, and Double Delta Wings During Dynamic Pitching," AIAA Paper 97-1930 (to be presented).

A. Plotkin
Associate Editor

Concentration Measurements in Experimental Microbursts

Abbas A. Alahyari* and Ellen K. Longmire†
University of Minnesota, Minneapolis, Minnesota 55455

Introduction

ATMOSPHERIC microbursts have been recognized as a cause of aircraft accidents for more than 15 years.[1] Since that time, observational, numerical, and experimental studies have investigated microburst behavior and structure.[2–4] Recent studies have employed small-scale laboratory experiments to examine the propagation behavior and vortex dynamics of atmospheric microbursts.[5,6] Microbursts were simulated by releasing small volumes of heavy fluid into a less dense ambient. For sufficiently large Reynolds numbers, experimental and atmospheric microbursts behaved similarly. Specifically, the large-scale structure, propagation velocity, and maximum velocity could be interrelated by choosing length and time scales based on the appropriate equations of motion.

Whereas knowledge of the velocity field can be invaluable in identifying and surviving a microburst, knowledge of the temperature field can provide a useful secondary tool. Because microbursts are driven primarily by evaporational cooling, microburst occurrences are typically associated with a local decrease in temperature.[4] Further, it is expected that the greater the temperature drop, the stronger

Received May 4, 1996; revision received Nov. 13, 1996; accepted for publication Nov. 27, 1996; also published in *AIAA Journal on Disc,* Volume 2, Number 2.

*Graduate Research Assistant, Department of Aerospace Engineering and Mechanics; currently Postdoctoral Associate, Idaho National Engineering Laboratory, P.O. Box 1625, Idaho Falls, ID 83415-3885.

†Associate Professor, Department of Aerospace Engineering and Mechanics, 110 Union Street SE. Member AIAA.

the wind speeds generated. Current infrared sensors are capable of measuring such temperature drops ahead of an aircraft.[7] However, a need remains for practical and reliable relationships that can utilize temperature measurements, either alone or in combination with velocity measurements, to predict wind-shear hazard.

Because the large structures in experimental microbursts scale to those observed in atmospheric microbursts and because mixing is driven by large-scale motion rather than small-scale diffusion, it is expected that experimental and atmospheric microbursts would have similar mixing characteristics. Thus, the local concentration of heavy fluid in an experimental microburst can be related to regions of low temperature in an atmospheric one. Concentration measurements can be employed to examine relationships between local temperature decreases and expected wind velocities. The local concentration of heavy fluid in experimental microbursts was determined using planar laser-induced fluorescence. The evolution of concentration fields and correlations between concentration and velocity were investigated.

Experimental Technique

Isolated microbursts were simulated by releasing cylindrical slugs of heavy fluid (aqueous potassium phosphate solution) into a large volume of less dense fluid (aqueous glycerol solution). The heavy fluid impacted on a horizontal surface that represented the ground. A detailed description of the experimental arrangement and scaling is given by Alahyari and Longmire.[6] The equivalent spherical radius R_0 of the heavy fluid was 0.039 m, the density difference $\Delta\rho/\rho$ was 0.03, the time scale $T_0 = (R_0\rho/g\Delta\rho)^{1/2}$ was 0.36 s, and the velocity scale $V_0 = R_0/T_0$ was 0.11 m/s. The initial height measured from the bottom of the release cylinder was $3.81\,R_0$.

The flowfield was illuminated with pulsed light from a frequency-doubled Nd:YAG laser. The emitted beam was converted into a vertical sheet that intersected the microburst centerline. Rhodamine 6G was added to the heavier microburst fluid. At low concentrations, the intensity of light fluoresced by Rhodamine 6G varies approximately linearly with concentration. The refractive indices of the lighter and heavier fluids were matched to avoid concentration-averaged regions within the measurement plane.[8]

Flow images were captured on Kodak Technical Pan film with a Nikon N8008s 35-mm camera. Each film frame was exposed to light from a single laser pulse. Prior to each run, calibration photographs were taken of known concentrations of the Rhodamine solution (100, 75, 50, 25, 12, and 6% volumes of dye-containing heavy fluid in ambient fluid solution). Calibration solutions were placed in a Plexiglas® container (7×7 cm in cross section) and photographed under the same conditions as the actual flow.

All film negatives were digitized to 8-bit resolution at 135 dpi with a Nikon scanner. Each calibration image was processed to obtain a curve relating pixel intensity to vertical location. (Variations in intensity along the laser path were small.) Image files then were processed to obtain concentration maps based on vertical location and intensity. Concentration values were found by interpolating between intensity values on neighboring calibration curves. The uncertainty in concentration values is estimated to be $\pm 10\%$.

Results

Figures 1 and 2 show sequences of velocity and concentration fields resulting from two microburst events. The velocity fields were obtained by particle image velocimetry.[6] Times after release for each sequence are $4.96T_0$, $6.06T_0$, and $7.16T_0$. As the microburst descends, a large vortex ring forms near the front as a result of baroclinic vorticity (Fig. 1a). In Fig. 2a, regions of mixed fluid develop along the unstable interface between the original two fluids. Near the leading edge of the downdraft, heavy fluid wraps around the primary vortex core. Ambient fluid is entrained upstream of the vortex core as well as upstream of smaller-scale shear instabilities trailing the core. Heavy fluid near the centerline is associated with large downward velocities.

At $6.06T_0$, the vortex ring has impacted on the bottom surface and is expanding radially. The volume of mixed fluid has increased substantially since the last frame. At this time, both vertical and

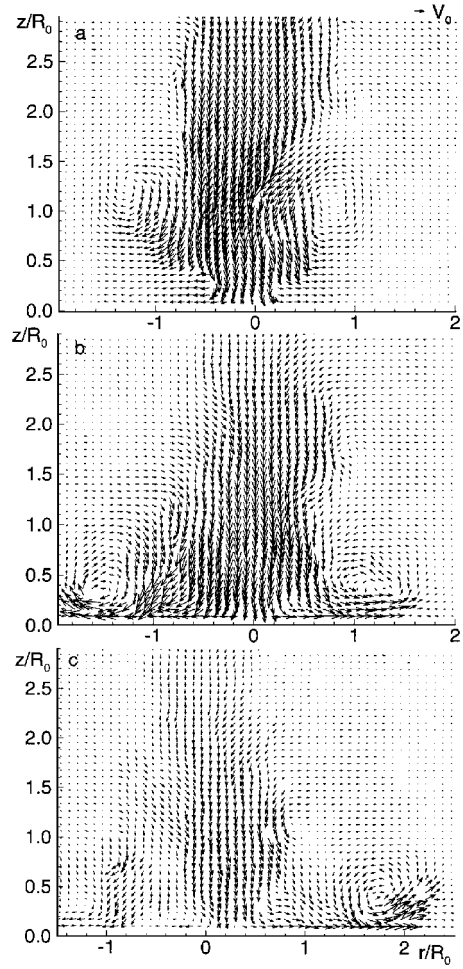

Fig. 1 Velocity vector fields: a) $4.96T_0$, b) $6.06T_0$, and c) $7.16T_0$ ($H_0 = 3.81\,R_0$, $Re = 3.6 \times 10^3$).

radial velocities are maximized ($\approx 2.5V_0$), and the microburst is considered most hazardous.[6] (Wind-shear "hazard" is caused by downflows and positive horizontal velocity gradients along the line of flight.) Large downward velocities exist throughout the downdraft column where concentration levels have decreased to less than 40%. Hence, a large amount of momentum is carried by entrained fluid.

High concentrations of heavy fluid are present in the vortex ring core and along the bottom surface where the concentration values range from 60 to nearly 100%. Most of the heavy fluid is associated with large radial velocities. These results are similar to the numerical simulations of Proctor.[4] A careful comparison of the velocity and concentration fields at $6.06T_0$ reveals that regions of peak concentration and peak radial velocity do not coincide. Peak radial velocities occur beneath the ring core at $1.2\,R_0$ from the centerline. In contrast, the relatively heavy fluid and thus peak temperature decreases are located near the centerline and at the very edge of the outflow. Also, most of the heavy fluid lies adjacent to the surface while peak horizontal velocities and gradients occur 0.05–0.2 R_0 above it. Thus, local temperature minima typically lie downstream of and beneath local velocity maxima.

In Fig. 2c, relatively heavy fluid continues to be swept upward from the surface by the vortex ring and wound into the core, while ambient fluid continues to be entrained from above. The peak concentration in the core has decreased, but remains above 50%. Vertical velocities near the centerline have decreased, and the largest velocity vectors are beneath and downstream of the vortex core. Thus, at this stage, the largest velocities lie close to an area of high concentration, but areas of high concentration do not necessarily correspond to high velocity. Furthermore, some of the strongest horizontal gradients (located upstream of the vortex core) are associated with 0% concentration level.

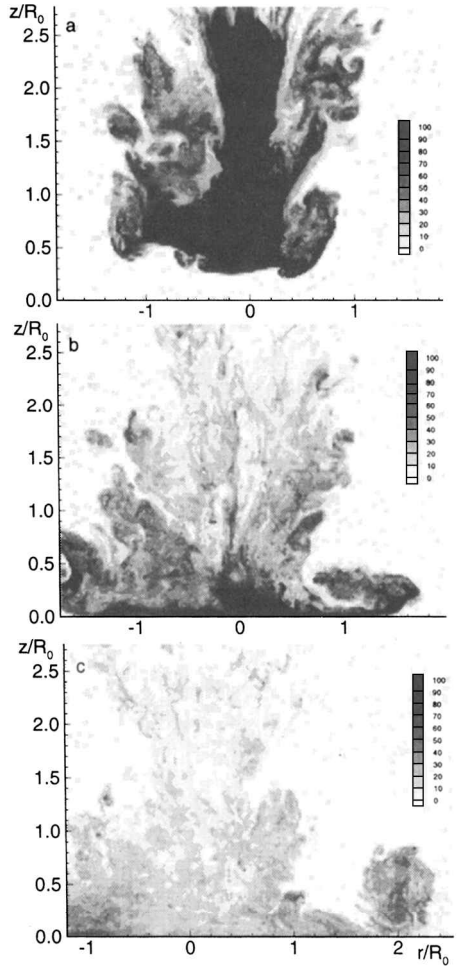

Fig. 2 Concentration fields: a) $4.96T_0$, b) $6.06T_0$, and c) $7.16T_0$ ($H_0 = 3.81R_0$, $Re = 3.6 \times 10^3$; levels represent percentage of heavy fluid).

The experimental concentration fields can be compared with interface contours computed by Lundgren et al.[5] using an inviscid vortex method. In the computations, heavy and light fluid were separated by an interface that stretched and rolled up as the microburst developed. All of the heavy fluid moved quickly to the leading edge of the downdraft, and ambient fluid was entrained from above and wrapped into the core. By the time of ring impact, the largest downdraft velocities were associated with this trailing ambient fluid. No heavy fluid was present in the wake of the ring. The experimental results are similar in that strong downflows persist after passage of the heavy fluid. In contrast, however, the experiment shows significant amounts of heavy fluid remaining in the downdraft column when the vortex ring impacts. Also, significant mixing occurs as a result of shear-driven instabilities at the interface between the light and heavy fluids. Different initial and boundary conditions (shape of initial microburst parcel, release mechanism, and vorticity distribution) in the experimental and numerical flows are probably the most important causes for differences in the results.

Conclusions

In experimental microbursts, heavy fluid wraps into a large vortex near the microburst front. Just before microburst impact, most of the heavy fluid trails the vortex and is associated with large downward velocities. The concentration of heavy fluid remains high in the vortex core and near the ground as the microburst expands radially. Local velocity maxima and gradient maxima are not always associated with heavy fluid, especially when the microburst is most hazardous. Because most ambient fluid is entrained from upstream, velocity maxima and strong horizontal gradients often trail local concentration maxima. Therefore, look-ahead sensing strategies for microburst prediction should not rely exclusively on single-point correlations between velocity and temperature measurements, but multiple-point correlations may be possible.

Acknowledgment

This work was funded by the National Science Foundation (CTS-9209948).

References

[1]Fujita, T. T., "Microbursts as an Aviation Wind Shear Hazard," *Proceedings of the AIAA 19th Aerospace Sciences Meeting* (St. Louis, MO), AIAA, New York, 1981, p. 9 (AIAA Paper 81-0386).

[2]Fujita, T. T., *The Downburst*, Univ. of Chicago Press, Chicago, IL, 1985.

[3]Wilson, J. W., Roberts, R. D., Kessinger, C., and McCarthy, J., "Microburst Wind Structure and Evolution of Doppler Radar for Airport Wind Shear Detection," *Journal of Climate and Applied Meteorology*, Vol. 23, No. 6, 1984, pp. 898–915.

[4]Proctor, F. H., "Numerical Simulation of an Isolated Microburst, Part 1: Dynamics and Structure," *Journal of Atmospheric Sciences*, Vol. 45, No. 21, 1988, pp. 3137–3160.

[5]Lundgren, T. S., Yao, J., and Mansour, N. N., "Microburst Modelling and Scaling," *Journal of Fluid Mechanics*, Vol. 239, 1992, pp. 461–488.

[6]Alahyari, A. A., and Longmire, E. K., "Dynamics of Experimentally Simulated Microbursts," *AIAA Journal*, Vol. 33, No. 11, 1995, pp. 2128–2136.

[7]Lewis, M. S., "Sensing a Change in the Wind," *Aerospace America*, Vol. 31, No. 3, 1993, pp. 20–24.

[8]Alahyari, A., and Longmire, E. K., "Particle Image Velocimetry in a Variable Density Flow: Application to a Dynamically Evolving Microburst," *Experiments in Fluids*, Vol. 17, No. 6, 1994, pp. 434–440.

G. Laufer
Associate Editor

Vortex Breakdown over Unsteady Delta Wings and Its Control

H. Yang* and I. Gursul†
University of Cincinnati, Cincinnati, Ohio 45221-0072

Introduction

THE unsteady aerodynamics of delta wings at high angle of attack has been the subject of several reviews.[1–3] In this Note, control of leading-edge vortices and vortex breakdown over a pitching delta wing with variable sweep are considered. When sweep-angle variations and pitching motion are combined with a proper phase angle, the amplitude of the variations of breakdown location becomes a minimum.

Several experimental studies of vortex breakdown in unsteady flows have shown that the dynamic response of the vortex breakdown location is characterized by time-lag effects. For example, the breakdown location exhibits a phase shift relative to wing motion for a periodically pitching delta wing.[4] The dynamic response of breakdown location is related to the two important parameters that determine the breakdown location: swirl angle and external pressure gradient outside the vortex core. It has been suggested that the dynamic response of vortex breakdown over a pitching delta wing can be explained by the variations of the external pressure gradient.[5] Unsteady pressure measurements indicate that the observed time lag of breakdown location is strongly linked to the external pressure gradient generated by the wing. Hall[6] showed that small external pressure gradients can be amplified along the core of the vortices, leading to a

Received April 29, 1996; revision received Oct. 25, 1996; accepted for publication Nov. 8, 1996; also published in *AIAA Journal on Disc*, Volume 2, Number 2.

*Graduate Student, Department of Mechanical, Industrial, and Nuclear Engineering.

†Assistant Professor, Department of Mechanical, Industrial, and Nuclear Engineering. Member AIAA.